

Investigation of Physicochemical Properties of Mo Carbide Utilizing Electron Spectroscopy

Eunkang Jeong, Juyun Park, and Yong-Cheol Kang[†]

Abstract

Molybdenum carbide (MoC_x) thin films (TFs) were deposited by reactive radio frequency (rf) magnetron co-sputtering in high vacuum chamber. We compared the properties of MoC_x thin films as the rf power changed on C target. The result of alpha step measurement showed that the thickness of the MoC_x TFs varied from 163.3 to 194.86 nm as C power was increased from 160 to 200 W. The crystallinity of MoC_x such as b- Mo_2C , Mo_2C , and diamond like carbon (DLC) structures were observed by XRD. The oxidation states of Mo and C were determined using high resolution XPS spectra of Mo 3d and C 1s were deconvoluted. Molybdenum was consisted of Mo, Mo^{4+} , and Mo^{6+} species. And C was deconvoluted to C-Mo, C, C-O, and C=O species.

Keywords : Moc, Thin film, co-sputtering, DLC, XPS.

1. Introduction

Molybdenum carbide (MoC_x) has been applied in many fields^[1-7] because of its hardness and resistivity^[1,8]. MoC_x could be applied for catalyst as well because of its morphology like noble metal^[7]. The most of works for the synthesis of MoC_x have been used chemical vapor deposition and physical vapor deposition methods with the assistance of CH_4 as a reactive gas^[1,2,5,6,9-13].

Ji *et al.* prepared MoC_x thin films by means of sputtering of Mo target with inductively coupled rf plasma chemical vapor deposition assisted with CH_4/Ar at various sputtering current on Mo target^[14]. The phases of MoC_x thin film were $\text{MoC}(100)$ and DLC structure. And X-ray photoelectron spectroscopy (XPS) spectra was showed molybdenum carbide phase. In Raman experiment, D peak was shift to G peak as sputtering current was increased. So, intensity ratio of D/G was decreased. Intensity ratio of D/G is the indirect measure of sp^3 bond. The decrease of D/G ratio implied that the sp^3 bond of C was decreased on MoC_x thin films.

Roughness of the MoC_x was increased as sputtering current increased.

Alberto *et al.* made Mo_2C catalyst. An appropriate amount of ethanol was added MoCl_5 , for forming the metal orthoesters^[7]. Metal orthoesters was combined with solid ureas and urea gels, and heated at 800°C with nitrogen gas flow for 3 hr. Mo_2C phase was investigated by X-ray diffraction (XRD).

This paper reports the results of fabrication of MoC_x thin films on Si(100) substrate using rf magnetron co-sputtering using C and Mo targets. The MoC_x thin films were obtained at various rf powers on C target without reactive gas in high vacuum chamber (HV). We investigated the chemical environment of MoC_x thin films using XPS, the crystallinity using XRD, electrical properties using four point probe measurement, and the surface free energy (SFE) of the thin films employing contact angle measurement using distilled water (DW) and ethylene glycol (EG).

2. Experimental

MoC_x thin films were deposited on p-type Si(100). The Si wafer was cleaned with acetone and dried with nitrogen gas prior to transfer into the co-sputtering chamber. MoC_x was deposited by rf (13.56 MHz) magnetron co-sputtering method. Substrate temperature was

Department of Chemistry, Pukyong National University, 45 Yongso-ro, Nam-Gu, Busan 48513, Korea

[†]Corresponding author : yckang@pknu.ac.kr

(Received: August 19, 2020, Revised: August 29, 2020,

Accepted: September 4, 2020)

maintained at 60°C. And the substrate was rotated at 12 rpm for uniform deposition. For co-sputtering method, two targets were used; C and Mo. Both sputtering targets have 50 mm of diameter and 5 mm in thickness. The rf power on Mo target was optimized at 30 W for whole co-sputtering process. Then, the power on C target was varied 160 to 200 W with a 10 W increment. From hereafter, the MoC_x thin films obtained at X W of rf power on C target will be referred as MoC-X. Ar gas was used for sputtering gas without using reactive gas such as CH₄. The flow rate of Ar was fixed at 20 sccm which was controlled with a mass flow controller. Base pressure of the co-sputtering chamber was kept less than 7×10^{-7} Torr, and working pressure was maintained 24.9 to 25.2 mTorr by a rotary vane pump (RP) and a turbo molecular pump (TMP). The co-sputtering chamber was cleaned before co-sputtering process. The chamber was pre-heated at 30 °C for 30 min to evacuate the contaminants before every experiment. Pre-sputtering was performed for 10 min to clean the targets and stabilize plasma as the shutters were closed. After the pre-sputtering, co-sputtering for deposition of MoC_x was carried out for 1 hr as the shutters opened.

The thickness of MoC_x thin films were measured with a surface profiler (alpha step-500, Tencor, USA). The crystallinity of MoC_x thin films was investigated by XRD (X'pert –MPD system, Philips, Netherland) with glancing mode. Cu K α radiation and 0.05 degree of step size were applied for XRD study. The chemical environment of MoC_x thin films was investigated by XPS (ESCALab MKII, VG, UK). Mg K α X-ray source (1253.6 eV) was used for the XPS. The base pressure of the XPS system was kept around 3×10^{-10} Torr by a RP, a TMP, two ion pumps (IP), and a Ti-sublimation pump (TSP). The survey XPS spectra were collected with a pass energy of 100 eV, dwell time of 100 ms, and an energy step of 0.5 eV. The XPS survey spectra were obtained after scanning 4 times to increase the signal to noise ratio. High resolution XPS spectra were taken with a pass energy of 50 eV, an energy step of 0.05 eV, scanned 9 times, and the other of parameters were kept the same as the survey scan. For detailed chemical information of MoC_x thin films, the high resolution XPS spectra of C and Mo were deconvoluted by using XPSPEAK41 software (ver 4.1) in 30% of Gaussian/Lorentzian ratio. The electrical properties were measured with a 4-point probe system (MCP-T600,

Loresta, Netherlands). And contact angles of DW and EG were measured to determine the surface free energy of MoC_x films using home-made contact measurement system.

3. Results and Discussion

Fig. 1 shows the thickness of MoC_x thin films deposited on p-type Si substrate at various rf powers on C target (160~200 W) and fixing rf power on Mo target (30 W) for 1 hr. The thickness of the MoC_x thin films were measured by alpha step measurement and the measured thickness were averaged after Grubbs test at 95% of confidence level^[15]. As shown in Fig.1, the thickness of MoC_x thin film was increased from 163.27 to 194.68 nm when the rf power on C target increased from 160 to 200 W, respectively. This phenomenon can be explained that the power on C affected to the velocity of Ar ion in plasma and sputtering rate of carbon was increased. This caused the thickness of the MoC_x thin films was increased as the rf power of carbon target increased.

The crystallinity of MoC_x thin films was investigated with XRD as shown in Fig. 2. The most intense peak in all spectra appeared at about the diffraction angle of 55.41° is assigned for Si(311) [JCPDS #80-0018] of the substrate. The crystalline phase of carbon was observed as diamond like carbon (DLC) phase. The DLC phase is assigned for DLC(107) [JCPDS #79-1473]. The intensity of the phase was increased as rf power increased. Two MoC_x crystalline phases were assigned

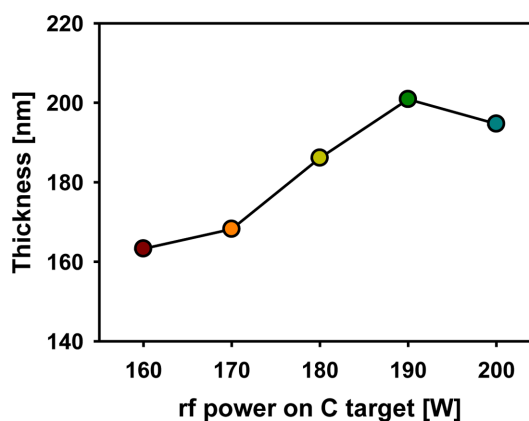


Fig. 1. Thickness of MoC_x thin films as a function of rf power on C target.

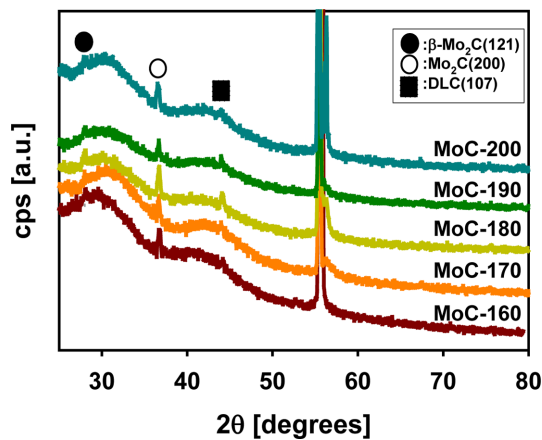


Fig. 2. Crystallinity of MoC_x thin films as C target sputtering power change.

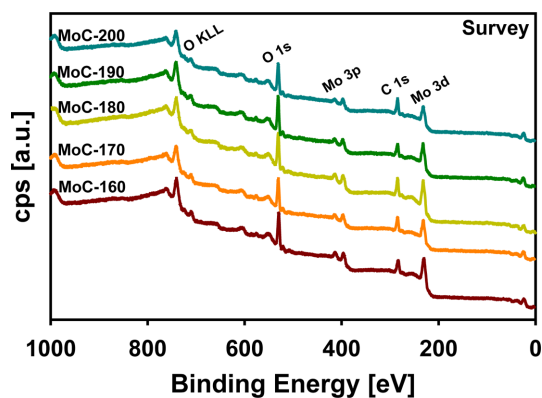


Fig. 3. XPS survey spectra of MoC_x thin films

for β -Mo₂C(121) [JCPDS #45-1013] and Mo₂C(200) [JCPDS #79-0744] at the diffraction angles of 28.12° and 36.63°, respectively. The intensity of β -Mo₂C(121) phase was slightly decreased as rf power increased. Mo₂C(200) phase at 36.63° was slightly increased as rf power increased.

Fig. 3 shows the XPS survey spectra of MoC_x thin films obtained at different rf powers on C target. The characteristic XPS peaks of O, C, and Mo were observed at the binding energies of 531.0, 284.1, and 231.28 eV, respectively. The XPS peak at 398.4 eV was assigned as Mo 3p_{5/2}. Although pure Ar gas was used for co-sputtering, XPS peak of O was detected. The oxygen could be originated from the residual oxygen species in the co-sputtering chamber such as H₂O and/or CO₂. This is an indirect clue of the formation of

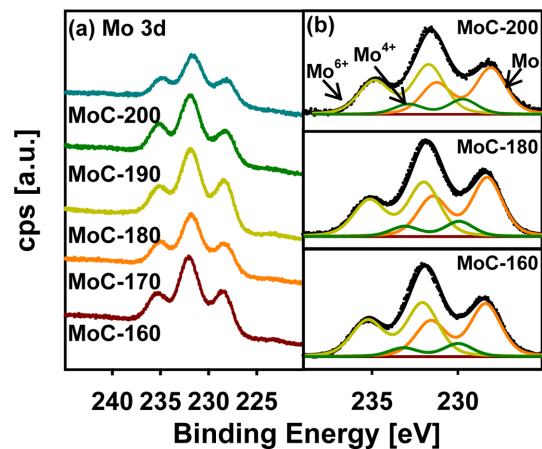


Fig. 4. (a) High resolution XPS Spectra of Mo 3d in MoC_x thin films and (b) tentative deconvoluted Mo 3d spectra

MoC_x thin films. In order to identify the chemical environment of MoC_x thin films, the high resolution XPS spectra of C 1s and Mo 3d were taken.

Fig. 4(a) shows the high resolution XPS spectra of Mo 3d in MoC_x thin films. Mo 3d XPS spectra of MoC_x thin films was apparently looked triplet peaks because Mo species with different oxidation states were combined. So, for the identification of the oxidation states of Mo, Mo 3d peaks were deconvoluted using XPSPEAK41. Fig. 4(b) shows the representative deconvoluted XPS spectra of Mo 3d. As shown in Fig. 4(b), the deconvoluted Mo 3d peaks were consisted of three peaks. The peak 1 (lowest BE) was assigned for Mo metallic phase. Peak 2 (middle BE) was assigned for Mo⁴⁺ phase. Peak 3 (highest BE) was assigned for Mo⁶⁺ phase^[16].

Fig. 5(a) is the high resolution XPS spectra of C 1s of MoC_x thin films obtained at various rf powers on C target. As shown in Fig. 5(a), the peak was not symmetric, so the C 1s peaks were deconvoluted. As shown Fig. 5(b), deconvoluted spectra of C 1s was consisted of four peaks, C-Mo, C, C-O, and C=O^[16]. C peaks, the peak at the highest BE was centered at 234.6 eV. So that can used as the reference of the XPS spectra. The intensity of MoC peak was increased as the rf power increased. This phenomenon was affected by the applied rf power like the thickness. The higher power on C target, the more carbon ion was sputtered. Therefore more MoC was formed.

Fig. 6 shows the electrical properties of MoC_x thin films. The conductivity of the MoC_x thin film was

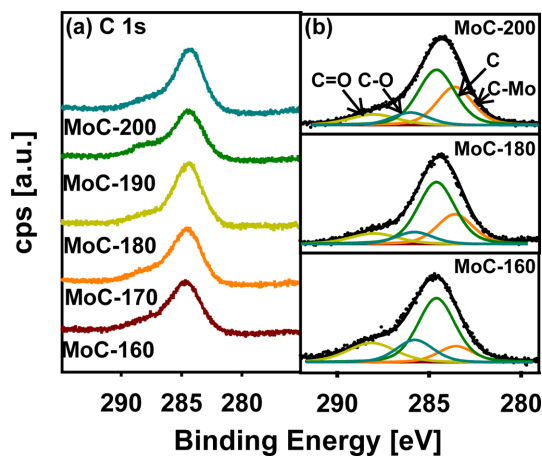


Fig. 5. Spectra of C 1s in MoC_x thin films and deconvolution data

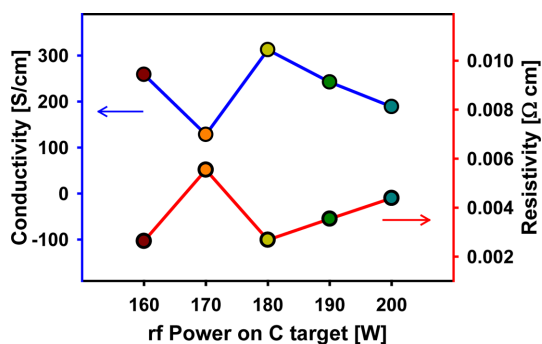


Fig. 6. Electrical properties of MoC_x thin films.

affected Mo atomic ratio. The conductivity was decreased from 258.68 to 128.10 S/cm as Mo ratio was decreased from 19.23% (MoC-160) to 15.86% (MoC-170). And then as the rf power increased from 170 to 180 W, the conductivity was increased from 128.10 to 312.44 S/cm. This phenomenon can be explain that the Mo is more effective to conductivity. The resistivity of MoC_x is inverse propensity to the conductivity.

Surface free energy of MoC_x thin films was shown at Fig. 7. The polar energy of MoC_x increase as rf power was increased. On the contrary, dispersive energy of the MoC_x is decreased as rf power increased. Then, the total SFE was decreased as the rf power increased.

4. Conclusion

The thickness of the MoC_x thin films has increased

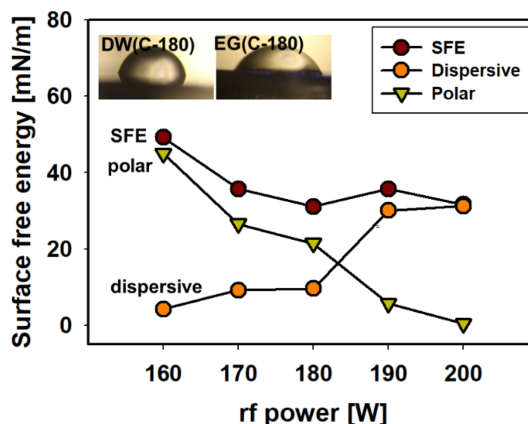


Fig. 7. Surface free energy of MoC_x thin films.

as rf power on the C target increased which was measured by alpha step measurement system. MoC_x has the three phases of crystallinity, DLC(107), β - Mo_2C (121), and Mo_2C (200). The intensity of Mo_2C (200) was increased as rf power increased. From XPS survey spectra, C-Mo species in C 1s was increased as rf power increased. And Mo 3d peak was consist of the Mo, Mo^{4+} , and Mo^{6+} . Atomic ratio of Mo was decreased as rf power increased. On the contrary, C was increased as rf power increased. Atomic ratio of Mo affects the conductivity of MoC_x . SFE of the MoC_x thin films was decreased as rf power increased.

Acknowledgment

This work was supported by a Research Grant of Pukyong National University (2019, CD2019-0628)

References

- [1] C. C. Tripathi, M. Kumar, and D. Kumar, Bull. Mater. Sci., 34, 1611 (2011).
- [2] Q. Liu, X.P. Wang, F.J. Liang, J.X. Wang, and Q.F. Fang, Mater. Res. Bull., 41, 1430 (2006).
- [3] E. Bertran, C. Corbella, A. Pinyol, M. Vives, and J.L. Andujar, Diam. Relat. Mater., 12, 1008 (2003).
- [4] G. D. Temmerman, M. Ley, J. Boudaden, and P. Oelhafen, J. Nucl. Mater., 337, 956 (2005).
- [5] X. He, W. Li, and H. Li, Mater. Sci. Eng. B-Adv., 31, 269 (1995).
- [6] Z.G. Yuan, J.F. Yang, Z.J. Cheng, X.P. Wang, and Q.F. Fang, Surf. Coat. Tech., 231, 14 (2013).

- [7] A. Villa, S. Campisi, C. Giordano, K. Otte, and L. Prati, *ACS Catal.*, 2, 1377 (2012).
- [8] A. Hanif, T. Xia., A. P. E. York, J. Sloan, and M. L. H. Green, *Chem. Mater.*, 14, 1009 (2002).
- [9] L. Ji, H. Li, F. Zhao, W. Quan, J. Chen, and H. Zhou, *Appl. Surf. Sci.*, 255, 4180 (2009).
- [10] H.Y. Chen, L. Chen, Y. Lu, Q. Hong, H.C. Chua, S.B. Tang, and J. Lin, *Catal. Today*, 96, 161 (2004).
- [11] K. Karlsruhe, *J. Low. Temp. Phys.*, 69, 257 (1987).
- [12] C. Corbella, M. Vives, A. Pinyol, E. Bertran, C. Canal, M. C. Polo, and J. L. Andujar, *Surf. Coat. Tech.*, 177, 409 (2004).
- [13] K. Baba and R. Hatada, *Surf. Coat. Tech.*, 196, 207 (2005).
- [14] L. Ji, H. Li, F. Zhao, J. Chen, and H. Zhou, *Diam. Relat. Mater.*, 17, 1949 (2008).
- [15] D. C. Harris, *Quantitative Chemical Analysis*, 8th ed., W. H. Freeman and Company: New York, 2010.
- [16] C. Anandan, L. Mohan, and P. D. Babu, *Appl. Surf. Sci.*, 296, 86 (2014).
- [17] C. A. Wolden, A. Pickerell, T. Gawai, S. Parks, J. Hensley, and J. D. Way, *ACS appl. Mater. Interfaces*, 3, 517 (2011).
- [18] C. C. Tripathi, M. Kumar, and D. Kumar, *Appl. Surf. Sci.*, 255, 3518 (2009).
- [19] E. Lucazeau, A. Deneuve, J. Fontenile, F. Brunet, and E. Gheeraert, *Diam. Relat. Mater.*, 5, 779 (1996).
- [20] C. Corbella, G. Oncins, M.A. Gomez, M.C. Polo, E. Pascual, J. Garcia-Cespedes, J.L. Andujar, and E. Bertran, *Diam. Relat. Mater.*, 14, 1103 (2005).
- [21] C. Blomfield, B. Tielsch, and L.Y.C. Tan, *J. Appl. Phys.*, 86, 4871 (1999).
- [22] E. L. Hasse, *J. Low. Temp. Phys.*, 69, 245, (1987).
- [23] N. S. Alhajri, D. H. Anjum, and K. Takanabe, *J. Mater. Chem., A*, 2, 10548 (2014).